2008

Discrete skyrmions in 2+1 and 3+1 dimensions

T Ioannidou

PG Kevrekidis
University of Massachusetts - Amherst, kevrekid@math.umass.edu

Discrete Skyrmions in 2+1 and 3+1 Dimensions

THEODORA IOANNIDOU[†1] and PANOS KEVREKIDIS[‡]

[†] *TAT, Eberhard Karls Universitat Tübingen, 72076 Tübingen, Germany*

[‡] *Department of Mathematics and Statistics, University of Massachusetts, Amherst, MA* $01003-4515$*, USA*

Emails: ti3@auth.gr

kevrekid@math.umass.edu

This paper describes a lattice version of the Skyrme model in $2+1$ and $3+1$ dimensions. The discrete model is derived from a consistent discretization of the radial continuum problem. Subsequently, the existence and stability of the skyrmion solutions existing on the lattice are investigated. One consequence of the proposed models is that the corresponding discrete skyrmions have a high degree of stability, similar to their continuum counterparts.

1 Introduction

Many attempts have been made in order to obtain the discrete analogue of given continuum systems that admit solitary wave solutions, so that their characteristics in the continuum be preserved in the lattice. One such characteristic for the topological systems is often the existence of the so-called Bogomolnyi bound [1]; while for the integrable ones it may be the existence of the Lax pair [2]. In the continuum, the stability of the topological solitons is often related to the existence of the energy bound while, the stability of the solitons in the integrable systems is related to the presence of an infinite number of conservation laws. However, in the lattice, only in a few cases the Bogomolnyi bound has been preserved [3, 4, 5] while it is even more difficult to define the lattice Lax pair (especially in higher dimensions) of the corresponding integrable system [2]. Moreover, the stability of the solitons in question is not guaranteed. Often, under discretization, the topological properties are essentially lost (as may be expected since topology is related to continuity). Lattice versions of these nonlinear

[1] *Permanent Adress:* School of Mathematics, Physics and Computational Sciences, Faculty of Engineering, Aristotle University of Thessaloniki, Thessaloniki 54124, Greece

wave bearing systems have been much studied (for purposes of numerical simulations [6] or regularization of the quantum field theory, or because they are of fundamental physical interest in their own right [7]).

For a given continuum model, there are many different discrete analogues which reduce to it in the continuum limit. The object of this paper it to present a lattice version of the Skyrme model in $2+1$ and $3+1$ dimensions. The Skyrme model is a popular model of the dynamics of pions and nucleons, incorporating the former as its fundamental pseudo-Goldstone field and the latter as topological solitons. Its continuum version has been widely studied using numerical and analytical methods (for more details, see for example, Ref. [8]). Its lattice formulation is of some importance since the model is non-renormalizable in perturbation theory and thus, existing treatments of the model are semiclassical (quantizing only the collective degrees of freedom of the soliton). Full quantization of the theory requires a cutoff which can be attained by its lattice version.

The most interesting feature of the Skyrme model is the stability conferred on the soliton by the topology [9]. An open question is whether this stability is preserved on the lattice. In this paper, lattice skyrmions obtained within an appropriate discretization of the Skyrme model in $2+1$ and $3+1$ dimensions are typically found to be stable in our parametric investigations. This suggests that these discretizations bear some important features of their continuum counterparts, while being easier to handle from a numerical point of view.

Our presentation is arranged as follows. The next section reviews the baby Skyrme model and then reparametrizes the fields to impose radial symmetry. Only then is the model discretized, as shown in section 2.1; while in section 2.2, numerical results on the the existence and stability of a single (radially symmetric) baby skyrmion on the lattice are given. The case of soliton configurations in the Skyrme model in $3+1$ dimensions was dealt with in the same way in section 3. Finally, our conclusions are presented in section 4.

2 The Baby Skyrme Model

Let us begin with a brief review of the Skyrme model in $2+1$-dimensions (so-called baby Skyrme model). The Lagrangian density of the model is of the form

$$\mathcal{L} = \frac{1}{2}\partial_\alpha \boldsymbol{\phi}\, \partial^\alpha \boldsymbol{\phi} - \frac{\kappa}{4}(\partial_\alpha \boldsymbol{\phi} \times \partial_\beta \boldsymbol{\phi})(\partial^\alpha \boldsymbol{\phi} \times \partial^\beta \boldsymbol{\phi}) - \mu^2 \left(1 - (\boldsymbol{n}\cdot\boldsymbol{\phi})^2\right). \tag{2.1}$$

The field $\boldsymbol{\phi}$ is a map from $M^3 \to S^2$, where M^3 is the 3-dimensional Minkowski space with metric $\eta^{\alpha\beta} = \mathrm{diag}(1,-1,-1)$ and the target space S^2 is the 2-sphere of unit radius embedded in Euclidean 3-space. Therefore, the field $\boldsymbol{\phi}$ is a scalar 3-vector with norm one, i.e. $|\boldsymbol{\phi}|^2 = 1$. The constants κ, μ are free parameters which have the dimension of length and energy, respectively. The first term in (2.1) is the familiar $O(3)$ sigma model, the second term is the 2-dimensional analogue of the Skyrme term and the last term is the potential.

The presence of the potential in (2.1) ensures the existence of stable skyrmion solutions. There are two other options in literature for its form: i) the holomorphic model where the potential term is $(1+\boldsymbol{n}\cdot\boldsymbol{\phi})^4$ but stable skyrmions cannot be obtained and (ii) the old baby Skyrme model where the potential term is $(1-\boldsymbol{n}\cdot\boldsymbol{\phi})$ and stable non-radially symmetric skyrmions exist. The Lagrangian (2.1) corresponds to the new baby Skyrme model [10] which possess radially symmetric skyrmions. In [11], approximate analytic skyrmion solutions of the new baby Skyrme model were obtained by exploring its topological properties.

Finiteness of the energy requires the potential term to vanish at infinity, implying that $\lim_{r\to\infty} \boldsymbol{\phi}(t,x,y) = \boldsymbol{n}$ (where $r = \sqrt{x^2+y^2}$). For simplicity we choose $\boldsymbol{n}$ to be the vacuum state, that is $\boldsymbol{n} = (0,0,1)$. Thus a topological number exists since the field $\boldsymbol{\phi}$, due to the boundary conditions, can be considered as a map from $S^2 \to S^2$.

The topological charge is the homotopy invariant of the field

$$\deg[\boldsymbol{\phi}] = \frac{1}{4\pi}\int \boldsymbol{\phi}\cdot(\partial_x\boldsymbol{\phi}\times\partial_y\boldsymbol{\phi})\,dx\,dy. \tag{2.2}$$

and thus, conserved.

2.1 Discrete Baby Skyrmions

In order to obtain the discrete analogue of the baby Skyrme model we restrict our considerations to fields which are invariant under simultaneous rotations and reflections in space and

target space. Thus, we assume that the field $\boldsymbol{\phi}$ is of the hedgehog form

$$\phi_i = k_i \sin g(r,t) k_i, \quad \phi_3 = \cos g(r,t) \tag{2.3}$$

where k_i for $i = 1, 2$ is a unit vector given in terms of the azimuthal angle θ and the topological charge $N = \deg[\boldsymbol{\phi}]$ as $k_i = (\cos N\theta, \sin N\theta)$; and $g(r,t)$ is the real profile function which satisfies certain boundary conditions. Then, the respective energy functionals related to Lagrangian (2.1) are

$$E_{\rm kin} = \pi \int r\dot{g}^2 \left(1 + \frac{\kappa^2 N^2}{r^2} \sin^2 g\right) dr \tag{2.4}$$

$$E_{\rm pot} = \pi \int \left(r g_r^2 + \frac{\kappa^2 N^2}{r} g_r^2 \sin^2 g + \frac{N^2}{r} \sin^2 g + \mu^2 r \sin^2 g\right) dr. \tag{2.5}$$

The boundary conditions for the skyrmions are: $g(0,t) = \pi$ and $g(r,t) = 0$ as $r \to \infty$. Note that the first and third term in (2.5) corresponds to the static $O(3)$ sigma model energy; the second term corresponds to the 2-dimensional static Skyrme energy and the last one is the potential.

Hereafter, r becomes a discrete variable with lattice spacing h. So, the real-valued field $g(r,t)$ depends on the continuum variable t and the discrete variable $r = nh$ where $n \in Z^+$. Then, $g_+ = g((n+1)h, t)$ denotes forward shift and thus, the forward difference is given by $\Delta g = (g_+ - g)/h$. There are many possibilities for discretizing the above energy functionals. However, based on the approach introduced in [5] for the discretization of the $O(3)$ sigma model, we assume that

$$\begin{aligned} g_r &= \frac{2f(h)}{h} \sin\left(\frac{g_+ - g}{2}\right) \\ \sin g &= \frac{1}{f(h)} \sin\left(\frac{g_+ + g}{2}\right). \end{aligned} \tag{2.6}$$

The parameter $f(h)$ is an arbitrary function of the lattice spacing subject to the constraint $f(h) \to 1$ as $h \to 0$.

The origin must be treated in a special way since the functionals are not defined at $n = 0$. One possibility is to assume (following [5]) that at the origin we have

$$\begin{aligned} \left(r g_r^2\right)\Big|_{r=0} &= \left(\frac{N^2}{r} \sin^2 g\right)\Big|_{r=0} \\ &= \frac{2N}{h} \cos^2\left(\frac{g(h,t)}{2}\right). \end{aligned} \tag{2.7}$$

Then, the kinetic and potential energy of the discrete baby Skyrme model are defined by the following expressions

$$
\begin{aligned}
E_{\rm kin} &= \pi\sum_{n=1}^{\infty} nh^2\dot{g}^2\left\{1+\frac{k^2N^2}{n^2h^2f^2}\sin^2\left(\frac{g_++g}{2}\right)\right\}\\
E_{\rm pot} &= 4\pi N\cos^2\left(\frac{g(h,t)}{2}\right)\left[1+\frac{2\kappa^2f^2}{h^2}\cos^2\left(\frac{g(h,t)}{2}\right)\right]\\
&+ \pi\sum_{n=1}^{\infty}\left\{4nf^2\sin^2\left(\frac{g_+-g}{2}\right)+\frac{\kappa^2N^2}{nh^2}\sin^2\left(\frac{g_+-g}{2}\right)\sin^2\left(\frac{g_++g}{2}\right)\right.\\
&\left.+\frac{N^2}{nf^2}\sin^2\left(\frac{g_++g}{2}\right)+\frac{\mu^2nh^2}{f^2}\sin^2\left(\frac{g_++g}{2}\right)\right\}. \qquad (2.8)
\end{aligned}
$$

Note that, for discretizing the second term of the energy at the origin, a combination of formula (2.6) and (2.7) has been used. Actually, when this term is absent no stable lattice baby skyrmions can be obtained. Recall, that this term is the discrete analog of the Skyrme term which stabilizes the solution and apparently its presence is vital (even at the origin).

For $\kappa=\mu=0$ the model (2.8) becomes the discrete version of the $O(3)$ sigma model introduced in [5].

The lattice equations of motion obtained from the variation of the Lagrangian $L=E_{\rm kin}-E_{\rm pot}$ given by (2.8) are

$$
\begin{aligned}
&\ddot{g}\left[1+\frac{\kappa^2N^2}{h^2f^2}\sin^2\left(\frac{g_++g}{2}\right)\right]+\frac{\kappa^2N^2}{2h^2f^2}\sin(g_++g)\left(\frac{\dot{g}^2}{2}+\dot{g}\dot{g_+}\right)\\
&=\frac{N}{h^2}\sin g\left(1+\frac{4\kappa^2f^2}{h^2}\cos^2\frac{g}{2}\right)+\sin(g_+-g)\left[\frac{g^2}{h^2}+\frac{\kappa^2N^2}{4h^4}\sin^2\left(\frac{g_++g}{2}\right)\right]\\
&\quad-\sin(g_++g)\left[\frac{N^2}{4h^2f^2}+\frac{\mu^2}{4f^2}+\frac{\kappa^2N^2}{4h^4}\sin^2\left(\frac{g_+-g}{2}\right)\right],\ \ n=1
\end{aligned}
$$

$$
\begin{aligned}
&n\ddot{g}\left[1+\frac{\kappa^2N^2}{nh^2f^2}\sin^2\left(\frac{g_++g}{2}\right)\right]+\frac{\kappa^2N^2}{2h^2f^2}\left[\frac{\sin(g_++g)}{n}\left(\frac{\dot{g}^2}{2}+\dot{g_+}\dot{g}\right)-\frac{\sin(g+g_-)}{n-1}\frac{\dot{g}_-^2}{2}\right]\\
&=-\sin(g-g_-)\left[\frac{g^2}{h^2}(n-1)+\frac{\kappa^2N^2}{4h^4}\frac{1}{(n-1)}\sin^2\left(\frac{g+g_-)}{2}\right)\right]\\
&\quad+\sin(g_+-g)\left[\frac{g^2}{h^2}\,n+\frac{\kappa^2N^2}{4h^4}\frac{1}{n}\sin^2\left(\frac{g_++g}{2}\right)\right]\\
&\quad-\sin(g_++g)\left[\frac{N^2}{4f^2h^2}\frac{1}{n}+\frac{\mu^2}{4f^2}n+\frac{\kappa^2N^2}{4h^4}\frac{1}{n}\sin^2\left(\frac{g_+-g}{2}\right)\right]\\
&\quad-\sin(g+g_-)\left[\frac{N^2}{4f^2h^2}\frac{1}{(n-1)}+\frac{\mu^2}{4f^2}(n-1)+\frac{\kappa^2N^2}{4h^4}\frac{1}{(n-1)}\sin^2\left(\frac{g-g_-}{2}\right)\right],\ \ n>1.
\end{aligned}
$$

(2.9)

Next, our task is to study whether the aforementioned lattice equations admit skyrmion solutions and if this is the case investigate whether the topological properties of the solutions are maintained in the presence of the lattice.

2.2 Numerical Simulations

Our numerical procedure for obtaining the baby skyrmions is the following: we use a fixed point iteration to identify the static solutions of equations (2.9). An initial guess (for the fixed-point Newton iteration) in the form of an inverse trigonometric function (an arccos in the radial direction) is used which subsequently, after a few iteration steps, converges to an exact stationary solution. Examples of such solutions are shown in Figure 1 for $h = 0.65$ (left panels) and $h = 1.5$ (right panels). The results are obtained for the choices: $N = \kappa = \mu = f = 1$ (unless noted otherwise), although variations of the parameters do not significantly affect our conclusions presented below.

As expected, increase of h renders the solution more "coarse" (i.e., with a fewer sites participating in the "spine" of the skyrmionic structure). However, the stability of the wave is not crucially affected by the discretization, since the baby skyrmion remains stable throughout the range of parameters used in our numerical investigations. The stability is inferred from the eigenvalues of the relevant Jacobean of linearization around the solution. In particular, a linearization ansatz of the form:

$$g_n = g_n^{st} + \epsilon \exp(\lambda t) w_n \tag{2.10}$$

leads to an eigenvalue problem (to $\mathrm{O}(\epsilon)$, where ϵ is a formal small parameter) for the eigenvalue-eigenvector pair (λ, w_n); g_n^{st} represents the stationary solution obtained in the aforementioned Newton step. A solution is deemed to be stable if none of the eigenvalues $\lambda = \lambda_r + i\lambda_i$ of the linearization problem is found to have a strictly positive real part λ_r. A particularly peculiar feature of the model is that the second term on the left hand side of equations (2.9) does not contribute to the linearization (its lowest order contribution is $\mathrm{O}(\epsilon^2)$). This suggests that even if the solution is found to be linearly stable, the full dynamics of the system (2.9)

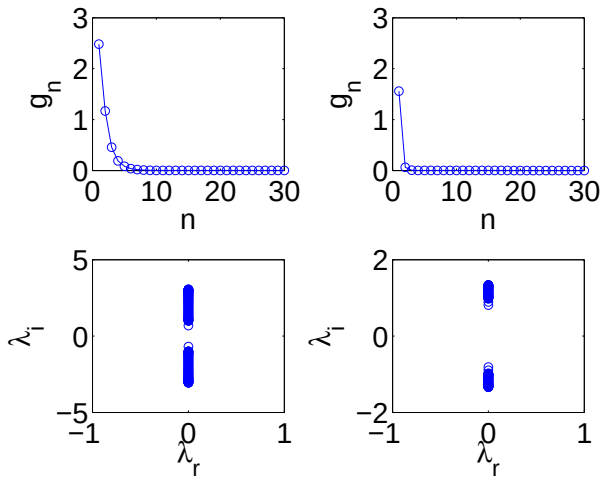

Figure 1: Typical profiles and stability results for the discrete baby skyrmions. The profile of the solution is shown in the top panels for $h = 0.65$ (left) and $h = 1.5$ (right). The corresponding spectral plane (λ_r, λ_i) of the eigenvalues $\lambda = \lambda_r + i\lambda_i$ of the linearization around the solutions is shown in the bottom panels.

should be considered, as it can, in principle, lead to nonlinear instabilities that cannot be detected at the linearization level. The results of the branch of solutions and their stability, obtained as a function of the lattice spacing h are summarized in Figure 2. The potential energy of the solutions, evaluated based on (2.8), reveals that the discretizations contributes towards decreasing the energy of the stationary solutions. The eigenvalues vary as a function of h, and interesting features such as bifurcations of internal modes (see e.g. [12, 13] and the references therein) arise e.g. for $h > 1.15$ from the bottom edge of the continuous spectrum. Additionally, a point spectrum (isolated) eigenvalue exists, which is also clearly discernible in the plots. Nevertheless, these do not appear to significantly affect the stability of the obtained discrete baby skyrmion structures.

Finally, we examine the dynamical evolution of the baby skyrmions to confirm the stability of the solutions obtained herein. We initialize the full dynamics of (2.9) with an exact baby skyrmion (for $h = 0.65$ in Figure 3) perturbed by a random (uniformly distributed) field of amplitude 5×10^{-3}. In Figure 3 the space-time evolution of the waveform and its persistence

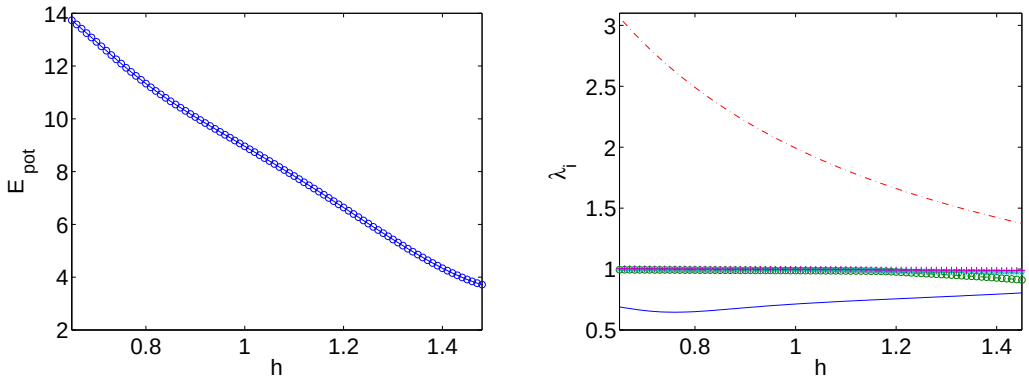

Figure 2: The left panel of the figure shows the potential energy of our exact static solutions given as a function of the lattice spacing h. In the right panel the principal (minimal, as well as maximal) imaginary parts of the eigenvalues of the linearization around the solutions are shown as a function of h.

in time (left panel) is presented, and it is obvious that despite the strength of the perturbation (which is, however, substantial) remains bounded during its time evolution in the right panel of the figure. This indicates that the baby skyrmions are robustly stable dynamical structures of the corresponding discrete equations.

Note that in [15], discrete 2-dimensional topological skyrmions have been constructed for a novel lattice version of the baby Skyrme model (i.e., the 2-dimensional topological Heisenberg model) but their stability was far weaker than the continuum ones since a fairly small perturbation caused their decay.

3 The Skyrme Model in $3+1$ Dimensions

The Lagrangian of the $SU(N)$ Skyrme model in $(3+1)$ dimensions can be written in terms of the currents $R_\mu = \partial_\mu U U^{-1}$ as

$$12\pi^2 \mathcal{L} = -\frac{1}{2}\mathrm{tr}\left(R_\mu R^\mu\right) - \frac{1}{16}\mathrm{tr}\left([R_\mu, R_\nu][R^\mu, R^\nu]\right) \tag{3.11}$$

where we have used scaled units of energy and length, and a $(+,-,-,-)$ signature for the space-time metric. The asymptotic value of the $SU(N)$ Skyrme field $U(x,t)$ has to tend to a

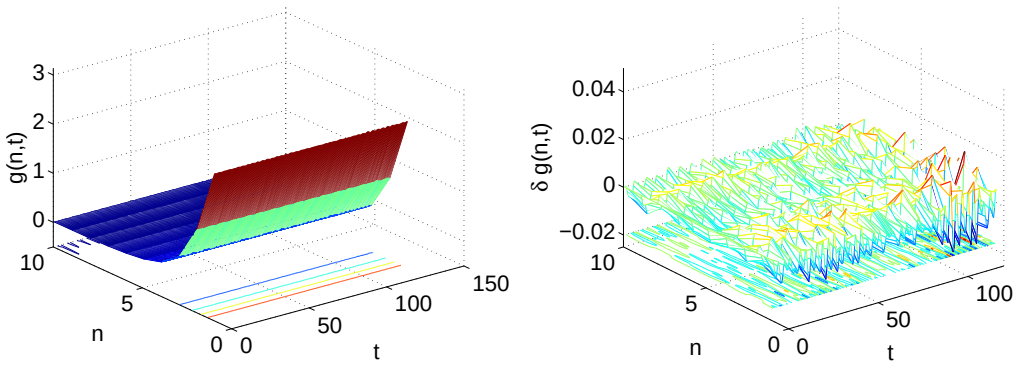

Figure 3: Space-time evolution of the baby skyrmion for $h = 0.65$ under an initial (random, uniformly distributed) perturbation of amplitude 5×10^{-3}. Note that despite the significant strength of the perturbation, the solution profile remains essentially intact (left panel), while the difference $\delta g(n,t) = g(n,t) - g(n,0)$ remains bounded (right panel) attesting to the robust stability of the discrete baby skyrmion.

constant matrix at spatial infinity, so that finite-energy configurations can exist.

The baryon density, whose spatial integral gives the integer-valued baryon number, is given by

$$24\pi^2 \mathcal{B} = -\varepsilon_{ijk} \mathrm{tr}\,(R_i R_j R_k)\,. \tag{3.12}$$

From the mathematical point of view these field configurations represent 3-dimensional topological solitons.

The model is not integrable and thus, with few exceptions, explicit solutions are hard to obtain. One way to overcome this problem is by expressing the Skyrme field in terms of harmonic maps of S^2 to CP^{N-1}. In particular, the idea of the rational map ansatz, introduced in [14] is to separate the radial and angular dependence of the Skyrme fields. Its $SU(N)$ generalization introduced in [16], expresses the Skyrme field in terms of a profile function $g(r)$ and a $N \times N$ Hermitian projector P that depends only on the angular variable as

$$U(r,\theta,\phi) = e^{2ig(r)(P-1/N)}. \tag{3.13}$$

The matrix P is a harmonic map from S^2 into CP^{N-1}. Hence it is convenient to map the sphere onto the complex plane via a stereographic projection in terms of the complex coordinate

$z = e^{i\phi}\tan(\theta/2)$ and its complex conjugate. In fact $P = (V \otimes V^\dagger)/|V|^2$ is given in terms of a N-component complex vector dependent on z and $\bar{z}$. For (3.13) to be well-defined at the origin, the radial profile function has to satisfy $g(0) = \pi$ while as $r \to \infty$, it is required that the Skyrme field has $\lim_{r\to\infty} g(r) = 0$.

In [14] it was shown that ansatz (3.13) describes field configurations for the $SU(2)$ model that are close to being solutions of the model. In particular, although the corresponding energies are slightly higher that the energies of the exact solutions (obtained numerically) the symmetries of the baryon and energy densities are the same. Also in [16], it was shown that when harmonic maps from S^2 to CP^{N-1} of the form (3.13) are considered, low-energy configurations of the $SU(N)$ Skyrme model can be derived. These configurations are more symmetrical than the $SU(2)$ ones but have higher energies. However, exact solutions with spherically symmetry may also be obtained from (3.13). They correspond to solutions of the $SU(2)$ and $SU(3)$ Skyrme model with baryon number $B = 1$ and $B = 0$ (topologically trivial solution), respectively.

Using (3.13) the energy of the Skyrme model simplifies to

$$E_{\rm kin} = \frac{1}{3\pi}\int \dot{g}^2(A_N r^2 + 2\mathcal{N}\sin^2 g)dr \tag{3.14}$$

$$E_{\rm pot} = \frac{1}{3\pi}\int \left(A_N r^2 g_r^2 + 2\mathcal{N}(g_r^2+1)\sin^2 g + \mathcal{I}\frac{\sin^4 g}{r^2}\right)dr \tag{3.15}$$

where

$$A_N = \frac{2}{N}(N-1) \tag{3.16}$$

$$\mathcal{N} = \frac{i}{2\pi}\int dzd\bar{z}\,{\rm tr}\left(|{\rm P_z}|^2\right) \tag{3.17}$$

$$\mathcal{I} = \frac{i}{4\pi}\int dzd\bar{z}(1+|z|^2)^2{\rm tr}\left([{\rm P_z},{\rm P_{\bar{z}}}]^2\right). \tag{3.18}$$

Note that the integrals $\mathcal{N}$ and $\mathcal{I}$ are independent of r. In particular, $\mathcal{N}$ corresponds to the energy of the 2-dimensional CP^{N-1} sigma model and is equal to the degree of the highest-order polynomial in z among the components of $V = R(z)$ (when being holomorphic) after all their common factors have been cancelled out.

Finally, the baryon number for this ansatz is

$$B = \frac{i}{2\pi}\int dzd\bar{z}\,{\rm tr}\left({\rm P}[{\rm P_{\bar{z}}},{\rm P_z}]\right) \tag{3.19}$$

which is the topological charge of the 2-dimensional CP^{N-1} sigma model.

In general, for V holomorphic, it was proved in [16] that $B = \mathcal{N} = n$ and $\mathcal{I} = n^2$ where $n = \deg(V)$. However, for the special $SU(3)$ non-topological solution the vector V is a function of z and $\bar{z}$ (i.e. non-holomorphic) . In this case, the baryon density is identically zero ($\mathcal{B} = 0$) and the solution describes a bound state of two skyrmions and two antiskyrmions and as such is unstable as it corresponds to a saddle point of the energy. Let us emphasize that the field configuration is a genuine (non-trivial) solution of the $SU(3)$ Skyrme model; while the corresponding parameters are $A_N = \frac{4}{3}$ and $\mathcal{N} = \mathcal{I} = 4$.

The Bogomolnyi-type argument for the Skyrme model gives the following lower energy bound

$$\begin{aligned} E_{\text{pot}} = \frac{1}{3\pi} \int \Bigg\{ & \left(\sqrt{A_N} r g_r + \sqrt{\mathcal{I}} \, \frac{\sin^2 g}{r} \right)^2 + 2\mathcal{N} \left(g_r + 1 \right)^2 \sin^2 g \\ & -2 \left(\sqrt{A_N \mathcal{I}} + 2\mathcal{N} \right) \sin g \partial_r (\cos g) \Bigg\} \, dr \\ \geq \; & \frac{1}{3} \left(2\mathcal{N} + \sqrt{A_N \mathcal{I}} \right), \end{aligned} \tag{3.20}$$

due to the boundary conditions of the profile function.

Baby skyrmions are topological solitons of the field theory which resembles the Skyrme model. Thus, in the following sections, we apply the techniques developed for discretizing the baby Skyrme model in the 3-dimensional Skyrme model.

3.1 Discrete Skyrmions

In what follows we present a lattice version of the Skyrme model by using the lower bound of the energy. Thus, following [4] we start with the same function $\sin g \partial_r (\cos g)$ as appears in (3.20) and reconstruct the inequality

$$\sqrt{A_N \mathcal{I}} \sin g \Delta \left(\cos g \right) = -D_n g_n \tag{3.21}$$

where $D_n \to \sqrt{A_N} r g_r$ and $F_n \to \frac{\sqrt{\mathcal{I}}}{r} \sin^2 g$ in the continuum limit $h \to 0$. The formula $\Delta(\cos g) = -2/h \sin\left(\frac{g_+ - g}{2}\right) \sin\left(\frac{g_+ + g}{2}\right)$ suggests the choices

$$D_n \;\; = \;\; \sqrt{A_N} (nh) \, \frac{2}{h} \, \sin \left(\frac{g_+ - g}{2} \right)$$

$$F_n \;=\; \sqrt{\mathcal{I}}\,\frac{1}{nh}\,\sin g \sin\left(\frac{g_+ + g}{2}\right). \tag{3.22}$$

Also, the origin must be treated in a special way since (3.22) are undefined at $n = 0$. One possibility is to arrange it so $D_0 + F_0 = 0$ implying that

$$D_0 = -F_0 = \frac{(A_N\mathcal{I})^{1/4}}{\sqrt{h}}\sqrt{g(h,t) - \pi}\,\sin g(h,t) \tag{3.23}$$

which follows for the discretization of the term: $\sqrt{A_N\mathcal{I}}\left[\Delta(g\sin^2 g) - g\Delta(\sin^2 g)\right]$. Note that, a direct discretization of (3.21) when $n = 0$ and assuming that $D_0 = -F_0$ is not possible since the terms are identically equal to zero due to the boundary condition $g(nh,t)|_{n=0} = \pi$. Thus, one possibility to overcome the problem is to discretize its counterpart term $\partial_r(g\sin^2 g) - g\partial_r(\sin^2 g)$. This way the non-trivial ansatz (3.23) is obtained.

Then, the potential energy of the lattice Skyrme model is given by

$$\begin{aligned} E_{\rm pot} \;&=\; 8\pi\sqrt{A_N\mathcal{I}}(g(h,t) - \pi)\sin^2 g(h,t) \\ &+\; 4\pi h\sum_{n=1}^{\infty}\left\{4A_N n^2\sin^2\left(\frac{g_+ - g}{2}\right) + \frac{\mathcal{I}}{n^2h^2}\sin^2 g\sin^2\left(\frac{g_+ + g}{2}\right)\right. \\ &\qquad \left. +2\mathcal{N}\left[\frac{4}{h^2}\sin^2\left(\frac{g_+ - g}{2}\right) + 1\right]\sin g\sin\left(\frac{g_+ + g}{2}\right)\right\}. \end{aligned} \tag{3.24}$$

Finally, the discrete version of the kinetic energy is

$$E_{\rm kin} = 4\pi h\sum_n\left[A_N\, n^2h^2 + 2\mathcal{N}\sin g\sin\left(\frac{g_+ + g}{2}\right)\right]\dot{g}^2. \tag{3.25}$$

The corresponding Euler-Lagrange equations obtained from the Lagrangian $L = E_{\rm kin} - E_{\rm pot}$ where the potential and kinetic energy are, respectively, given by (3.24) and (3.25), read

$$\begin{aligned} &\ddot{g}\left[A_N h^2 + 2\mathcal{N}\sin g\sin\left(\frac{g_+ + g}{2}\right)\right] + \mathcal{N}\dot{g}_+\dot{g}\sin g\cos\left(\frac{g_+ + g}{2}\right) \\ &+\mathcal{N}\dot{g}^2\left[\cos g\sin\left(\frac{g_+ + g}{2}\right) + \frac{\sin g}{2}\cos\left(\frac{g_+ + g}{2}\right)\right] \\ =\;& -\frac{\sqrt{A_N\mathcal{I}}}{h}\left[\sin^2 g + (g - \pi)\sin 2g\right] + A_N\sin(g_+ - g) \\ &-\mathcal{N}\left[\frac{4}{h^2}\sin^2\left(\frac{g_+ - g}{2}\right) + 1\right]\left[\cos g\sin\left(\frac{g_+ + g}{2}\right) + \frac{\sin g}{2}\cos\left(\frac{g_+ + g}{2}\right)\right] \\ &+\frac{2\mathcal{N}}{h^2}\sin(g_+ - g)\sin g\sin\left(\frac{g_+ + g}{2}\right) \end{aligned}$$

$$-\frac{\mathcal{I}}{2h^2}\left[\sin 2g\sin^2\left(\frac{g_+ + g}{2}\right) + \frac{\sin(g_+ + g)}{2}\sin^2 g\right], \quad n = 1 \tag{3.26}$$

$$\begin{aligned}
&\ddot{g}\left[A_N n^2 h^2 + 2\mathcal{N}\sin g\sin\left(\frac{g_+ + g}{2}\right)\right] + \mathcal{N}\dot{g}_+\dot{g}\sin g\cos\left(\frac{g_+ + g}{2}\right) \\
&+\mathcal{N}\dot{g}^2\left[\cos g\sin\left(\frac{g_+ + g}{2}\right) + \frac{\sin g}{2}\cos\left(\frac{g_+ + g}{2}\right) - \frac{\sin g_-}{2}\cos\left(\frac{g + g_-}{2}\right)\right] \\
= \;& A_N n^2\sin(g_+ - g) - A_N(n-1)^2\sin(g - g_-) \\
&-\mathcal{N}\left[\frac{4}{h^2}\sin^2\left(\frac{g_+ - g}{2}\right) + 1\right]\left[\cos g\sin\left(\frac{g_+ + g}{2}\right) + \frac{\sin g}{2}\cos\left(\frac{g_+ + g}{2}\right)\right] \\
&-\frac{\mathcal{N}}{2}\left[\frac{4}{h^2}\sin^2\left(\frac{g - g_-}{2}\right) + 1\right]\sin g_-\cos\left(\frac{g + g_-}{2}\right) \\
&-\frac{2\mathcal{N}}{h^2}\left[\sin(g - g_-)\sin g_-\sin\left(\frac{g + g_-}{2}\right) - \sin(g_+ - g)\sin g\sin\left(\frac{g_+ + g}{2}\right)\right] \\
&-\frac{\mathcal{I}}{2h^2}\left[\frac{\sin 2g}{n^2}\sin^2\left(\frac{g_+ + g}{2}\right) + \frac{\sin(g + g_-)}{2(n-1)^2}\sin^2 g_- + \frac{\sin(g_+ + g)}{2n^2}\sin^2 g\right], \quad n > 1.
\end{aligned} \tag{3.27}$$

In the next section, we will show that stable discrete skyrmion solutions of the aforementioned equations can be obtained numerically. In particular, the analogues of the $SU(2)$ $B = 1$ and $SU(3)$ $B = 0$ skyrmion configurations are constructed when the corresponding parameters are $A_N = 1$, $\mathcal{N} = \mathcal{I} = 1$ and $A_N = 4/3$, $\mathcal{N} = \mathcal{I} = 4$, respectively.

3.2 Numerical Solutions

The numerical existence and stability computations have been repeated similarly to the 2-dimensional case. The principal finding in this setting, as well, is that the skyrmion structures are found to be linearly stable, both in the $SU(2)$ and in the $SU(3)$ cases. In particular, examples of the profiles of the obtained structures and their linear stability are illustrated in Figure 4 for values of $h = 0.4$ (left panels) and $h = 1$ (right panels) for the two different parameter sets [top and bottom]. Notice the absence of any real eigenvalues showcasing the stability of the waves.

Using numerical continuation, with the spacing h as the relevant parameter, reveals that the structures remain stable as h is modified. The monotonically decreasing trends of the relevant principal imaginary eigenvalues with h are shown in Figure 5, together with the po-

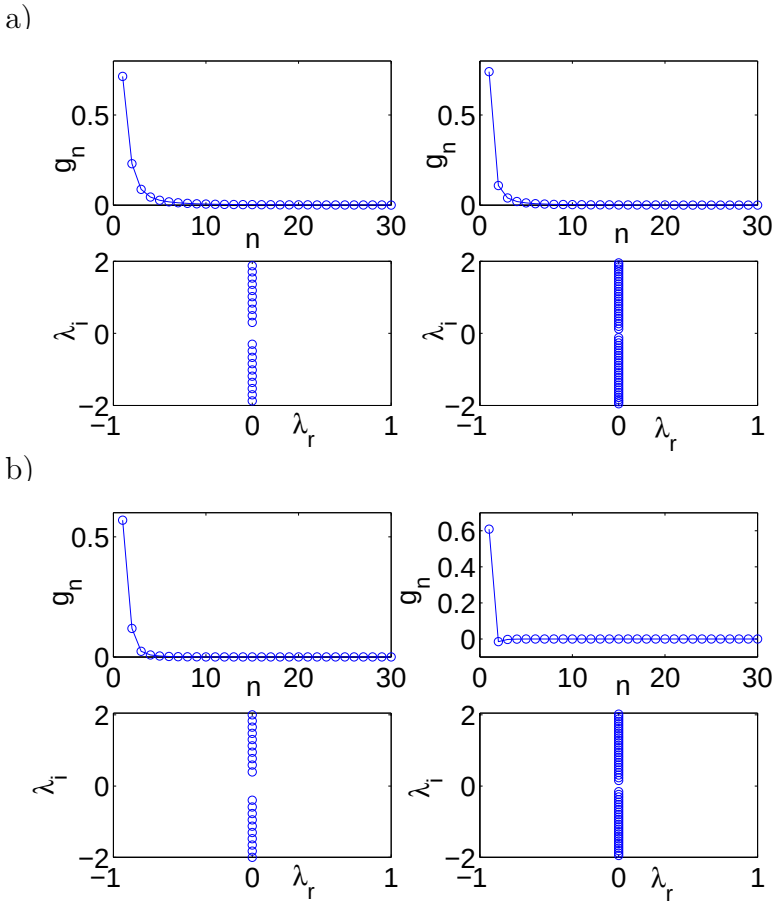

Figure 4: Same as Figure 1 but for the 3-dimensional case for a) the one $SU(2)$ skyrmion and b) for the topologically trivial $SU(3)$ skyrmion-antiskyrmion configuration. In each case the spatial profile of the skyrmion and the eigenvalues of its linearization are shown for $h = 0.4$ (left panels) and $h = 1$ (right panels).

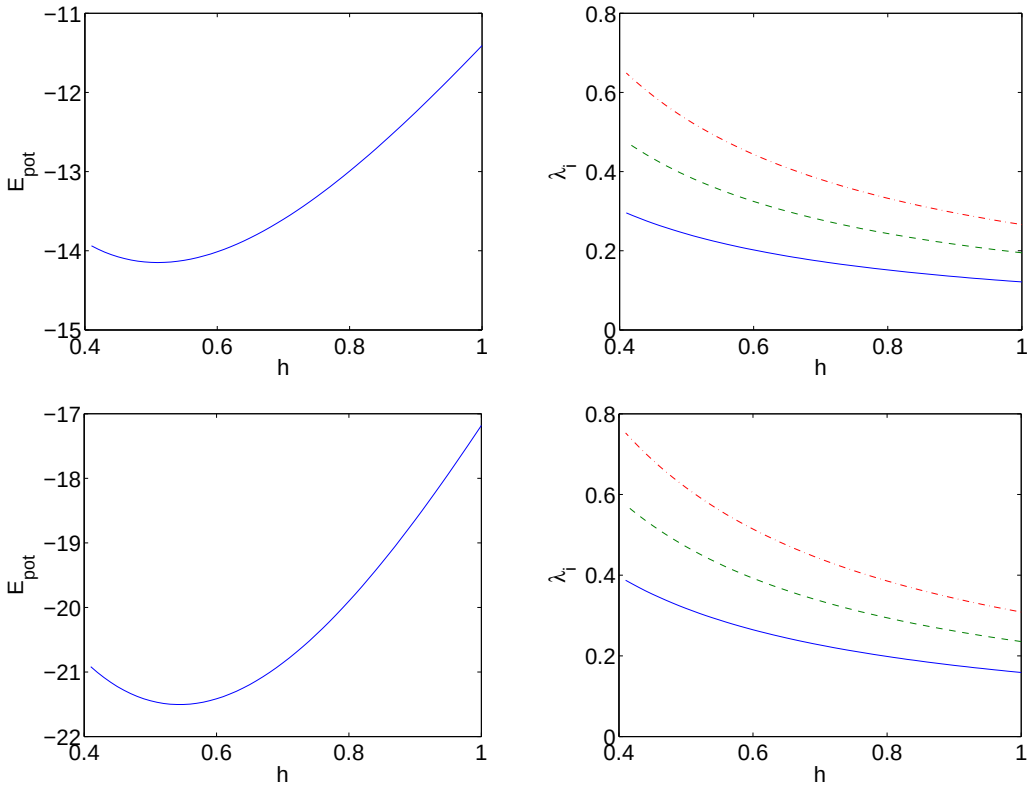

Figure 5: Same as the panels of Figure 2 but for the 3-dimensional case when $\mathcal{A}_N = \mathcal{I} = \mathcal{N} = 1$ (top row) and $\mathcal{A}_N = 4/3$ and $\mathcal{I} = \mathcal{N} = 4$ (bottom row). Notice that the right panels show the three lowest eigenvalues of the linear stability in each case.

tential energy dependence on the spacing. The latter quantity has a non-trivial non-monotonic dependence with a minimum around a given spacing (which is dependent on the parameters A_N, $\mathcal{N}$ and $\mathcal{I}$, but is both cases occurring near $h = 0.5$).

Finally, the numerical bifurcation analysis results were tested against the direct numerical integration of equations (3.27). These simulations are once again particularly relevant in this context as the dynamical evolution equation contain terms (such as the second term in the left hand side of (3.27)), which are not accounted for at the linear stability level [arising at $\mathrm{O}(\epsilon^2)$]; hence, it is important to check whether linearly stable solutions may be destabilized by such higher order effects. Our results for these simulations are summarized in Figure 6, where integration results are shown for times up to $t = 150$, with a strong perturbation to the exact

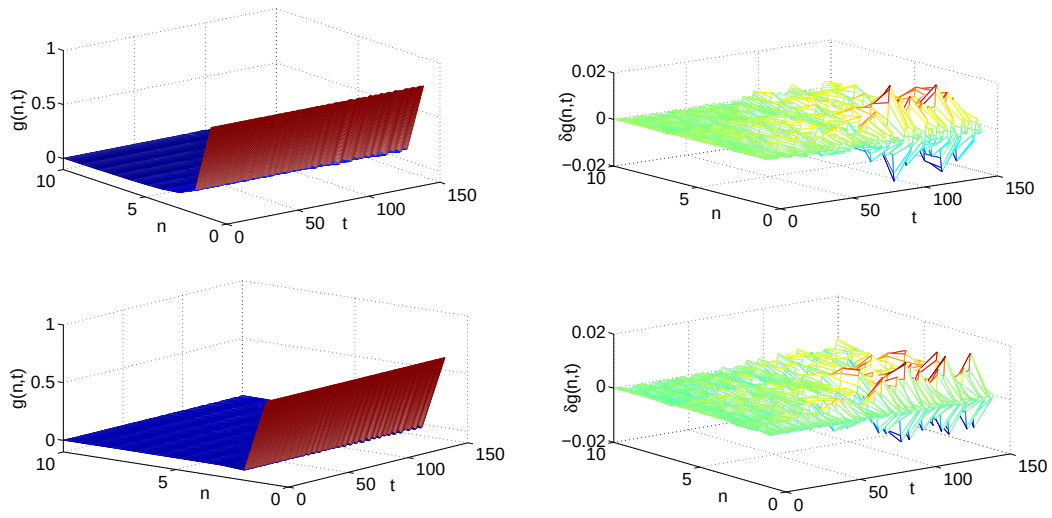

Figure 6: In a format similar to that of Figure 3, the figure presents direct numerical simulations of the cases with $\mathcal{A}_N = \mathcal{I} = \mathcal{N} = 1$ (top row) and $\mathcal{A}_N = 4/3$ and $\mathcal{I} = \mathcal{N} = 4$ (bottom row). The left panel shows in both cases the evolution of a skyrmion solution with $h = 1$ in space and time, while the right shows the deviation $\delta g(n,t) = g(n,t) - g(n,0)$ from the initial profile.

solution (for $h = 1$) of magnitude 10^{-3} being imposed as the initial condition. However, the relevant perturbation remains bounded for the duration of the simulation and even for times up to twice as large as the ones shown here. These results clearly indicate the robustness of the obtained solutions.

4 Conclusions

In this paper a novel discrete version of the Skyrme model in $2+1$ and $3+1$ dimensions is presented. It has been shown that both models admit discrete skyrmion solutions, similar to the continuum ones, which are well-behaved and remarkably stable, in the sense that they cannot be destroyed by small (or even not so small) perturbations. The discretization scheme is based on using polar coordinates and thus, the corresponding skyrmions are radially symmetric; and therefore, it is not possible to investigate their fully 2d or 3d dynamics. The

advantage of the version described in this paper, on the other hand, is that the lattice spacing can be relatively large, without compromising the stability of the solitons.

It should be instructive to produce discretizations of the full 2- and 3-dimensional systems, that are not restricted to radially-symmetric configurations, and to investigate the construction of the corresponding skyrmions. That way, the full dynamics of the discrete skyrmions can be considered, and directly tested against numerical simulations of the continuum ones [17, 18, 19]. The details of this program constitute an interesting direction for future study.

Acknowledgements

TI thanks University of Tübinger for a guest Professorship position. PGK gratefully acknowledges support from grants NSF-DMS-0505663, NSF-DMS-0619492 and NSF-CAREER.

References

[1] E.B. Bogomol'nyi, Sov. J. Nucl. Phys. **24**, 449 (1976).

[2] M.J. Ablowitz and H. Segur, Solitons and the Inverse Scattering Transform, SIAM (1981).

[3] R. A. Leese, Phys. Rev. D 40, 2004 (1989).

[4] J. M. Speight and R. S. Ward, Nonlinearity 7, 475 (1994).

[5] T. Ioannidou, Nonlinearity 10, 1357 (1997).

[6] M.J. Ablowitz, B.M. Herbst and C.M. Schober, J. Phys. A **34**, 10671 (2001).

[7] S. Flach and C.R. Willis, **295**, 181 (1998). S. Flach and A. Gorbach, preprint (2007).

[8] N. Manton and P. S. Sutcliffe, *Topological Solitons* (Cambridge University Press, 2004).

[9] W. J. Zakrzewski, *Low Dimensional Sigma Models* (Adam Hilger, Bristol 1989).

[10] T. Weidig, Nonlinearity 12, 1489 (1999).

[11] T. Ioannidou, V. B. Kopeliovich and W. J. Zakrzewski, J. Exp. Theor. Phys. 95, 572 (2002).

[12] Yu.S. Kivshar, D.E. Pelinovsky, T. Cretegny and M. Peyrard, Phys. Rev. Lett. 80, 5032 (1998).

[13] P.G. Kevrekidis and C.K.R.T. Jones, Phys. Rev. E 61, 3114 (2000).

[14] C. Houghton, N. Manton and P. Sutcliffe, Nucl. Phys. B 510, 587 (1998).

[15] R. S. Ward, Let. Math. Phys. 35, 385 (1995).

[16] T. Ioannidou, B. Piette and W. J. Zakrzewski, J. Math. Phys. 40, 6353 (1999); J. Math. Phys. 40, 6223 (1999).

[17] M. Peyrard, B. Piette and W. J. Zakrzewski, Nonlinearity 5, 563 & 585 (1992).

[18] B. M. A. G. Piette, B. J. Schroers and W. J. Zakrzewski, Nucl. Phys. B 439, 205 (1995).

[19] R. A. Battye and P. M. Sutcliffe, Phys. Let. B 391, 150 (1997).